

# Effects of Carbon Nanofibers on Crystalline Structures and Properties of Ultrahigh Molecular Weight Polyethylene Blend Fabricated Using Twin-Screw Extrusion

X. Ren,<sup>1,2</sup> X. Q. Wang,<sup>1</sup> G. Sui,<sup>2</sup> W. H. Zhong,<sup>2</sup> M. A. Fuqua,<sup>2</sup> C. A. Ulven<sup>2</sup>

<sup>1</sup>Department of Materials Science and Engineering, Beihang University, Beijing 100083, China

<sup>2</sup>Department of Mechanical Engineering and Applied Mechanics, North Dakota State University, Fargo, North Dakota

Received 27 June 2007; accepted 23 August 2007

DOI 10.1002/app.27354

Published online 19 November 2007 in Wiley InterScience (www.interscience.wiley.com).

**ABSTRACT:** Melt mixing in an extruder with polymers is an effective approach for forming nanocomposites, allowing mass production applications. The intent of this study is to investigate carbon nanofiber composites with ultrahigh molecular weight polyethylene (UHMWPE) matrix using the twin-screw extruder. To decrease the high viscosity of UHMWPE, a low density polyethylene (LDPE) was added into the UHMWPE. The effects of carbon nanofibers (CNFs) on the crystalline structures and properties of the nanocomposites were analyzed. The differential scanning calorimetry (DSC) and X-ray diffraction (XRD) measurements showed the addition of CNFs decreases the

degree of crystallinity, but does not impart significant effects on the crystalline structure of the UHMWPE/LDPE blend. Tensile test results showed that the nanocomposite with loading of 3 wt % CNFs had an increase of 38% in tensile strength and 15% in modulus. The thermal stability and thermal conductivity of UHMWPE/LDPE blends were also enhanced by the addition of CNFs. © 2007 Wiley Periodicals, Inc. *J Appl Polym Sci* 107: 2837–2845, 2008

**Key words:** UHMWPE; carbon nanofiber; the twin-screw extruder

## INTRODUCTION

Ultrahigh molecular weight polyethylene (UHMWPE) has many excellent properties, including high impact strength, low friction coefficient, good chemical resistance, and biocompatibility which make it a promising material for total joint replacement components.<sup>1–4</sup> However, mechanical and physical properties of UHMWPE still need to be improved in the areas of yielding, fracture, and fatigue behavior. These factors currently limit the longevity of UHMWPE as a bearing material used in total joint replacement components.<sup>1</sup> Therefore, it is desirable to further increase the mechanical properties and other properties such as the wear and friction resistance of UHMWPE materials.

To enhance various properties of UHMWPE, many programs have attempted to add fillers into UHMWPE to produce polymer matrix composites. These fillers had been reported to include carbon black,<sup>5</sup> graphite,<sup>6</sup> ceramic (kaolin),<sup>7</sup> metal,<sup>8</sup> and UHMWPE fibers.<sup>9</sup> Nanofillers have attracted much attention because of their higher specific area, higher

surface energy, and better mechanical properties than micro-fillers. It was reported that hydroxyapatite(HA)/UHMWPE nanocomposites with loading of 0.23 vol % HA nanoparticles showed the modulus was increased 10 times over that of neat UHMWPE.<sup>10</sup> However, there was little enhancement in yield strength and ductility of UHMWPE.

Carbon nanofibers (CNFs) are attractive nanofillers for polymer composites due to their high mechanical and thermal properties and relatively low cost compared with carbon nanotubes (CNTs). Polyethylene and polypropylene have been reinforced by CNFs.<sup>11–14</sup> The results showed that the mechanical properties of these polymers were improved with the addition of CNFs, leading to the proposition that CNF reinforced UHMWPE composites may have potential for application in total joint replacement. CNF/UHMWPE nanocomposite films have been studied and the results showed that the presence of up to 5 wt % CNFs led to a 10-fold toughness improvement over the pure UHMWPE film.<sup>15</sup> However, there are very few reports on mechanical properties of CNF/UHMWPE nanocomposite bulk materials other than CNF/UHMWPE nanocomposite films.

Many study results showed that the property improvement of nanocomposites is directly related to the dispersion levels of CNFs. To effectively disperse the CNFs in matrix polymers, miniaturized

Correspondence to: Dr. X. Q. Wang (wangxiaoqun@buaa.edu.cn).

internal mixer,<sup>12</sup> single screw extruder,<sup>14</sup> twin-screw blender,<sup>15</sup> and high speed mechanical agitator<sup>16</sup> have been applied. For mixing the CNFs specifically in UHMWPE, it has been reported that a twin-screw blender<sup>15</sup> was used. But the dispersion of CNFs in UHMWPE was still unsatisfactory, and processing technology that could result in uniform dispersion of CNFs and be suitable for mass production still needs to be developed.

Twin-screw extruders have been widely used in the processing of polymeric materials in industry, and produced uniform particle dispersion by the shear force in processing HA/UHMWPE nanocomposites.<sup>10</sup> However, high aspect ratio of CNFs and high viscosity of UHMWPE makes it difficult to process using the twin-screw extruder. Some solutions used to decrease the viscosity of UHMWPE include paraffin oil,<sup>10</sup> xylene,<sup>17</sup> decalin,<sup>9,18</sup> but these solutions affect the properties of the composites because it is hard to extract them out of the composites and clean the extruder. It is well known that blending with other thermoplastic polymers with low viscosity could improve the processibility of UHMWPE.<sup>19,20</sup>

The intent of this study is to investigate the fabrication and property enhancements of the CNF-reinforced UHMWPE nanocomposites prepared by using a newly acquired twin-screw extruder. Because of the high viscosity of UHMWPE, which made it initially difficult to be processed by the twin-screw extruder, a low density polyethylene (LDPE) was blended with UHMWPE for the ease of the processing. After several preliminary experiments, the blend with the highest ratio of the UHMWPE to LDPE that can be extruded using this lab size extruder was determined to be 30 : 70. A set of nanocomposites with different loadings of CNFs in this chosen polymer matrix blend of UHMWPE/LDPE were prepared using the twin-screw extruder. It should be noted here that although we have an on-going interest in investigating the pure UHMWPE nanocomposites, we conducted this initial work on nanocomposites with the UHMWPE/LDPE blend due to the inability to process pure UHMWPE in this manner using the extruder. We feel this work resulted in some interesting findings on the effects of CNFs on the subject crystalline structures and on the mechanical and thermal properties of UHMWPE which can lead to generalizations useful for future work.

## EXPERIMENTAL

### Materials

The medical grade of UHMWPE powder used in this study is GUR 1020<sup>®</sup> with molecular weight of  $3.5 \times 10^6$  g/mol and density of 0.935 g/cm<sup>3</sup> supplied by Ticona, KY. Figure 1 shows the morphology

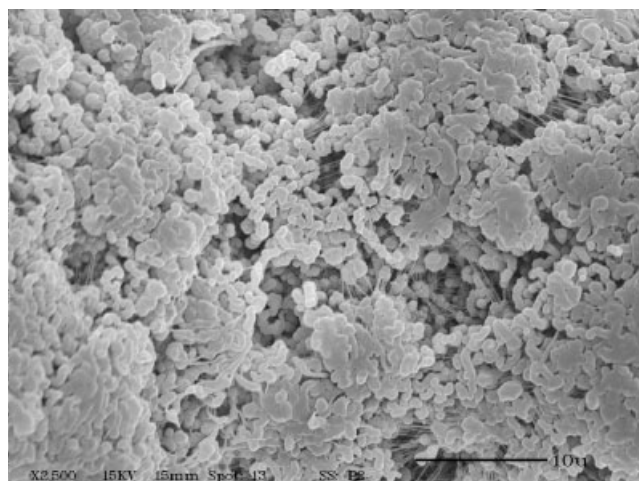


**Figure 1** The morphology of UHMWPE powder.

of the UHMWPE used in experiment. The LDPE powders were Marlex 1003<sup>®</sup> with the density of 0.917 g/cm<sup>3</sup> provided by the Chevron Philips, TX, USA. The CNFs used in this study are Pyrograf III<sup>®</sup> Carbon Fibers, HHT Grade, supplied by Pyrograf Products, OH, USA, which are 100–200 nm in diameter and 30–100 µm in length.

### Preparation of the nanocomposites

Blending UHMWPE with LDPE was at the ratio of 3 : 7, and then mixed with CNFs. The mixture was further compounded by the twin-screw extruder (Micro 18/GL-400, manufactured by the Leistritz Extruder, Germany) at the rate of 20 rpm. This twin-screw is capable of corotating, intermeshing, and counter-rotating for high shear compounding for polymer melts, with Micro-18 mm multimode and 40 to 1 L/D specially designed for fabricating nano- and biocomposites. The temperature profile from hopper to die was as follow: 135, 183, 193, 196, 202, 205, and 205°C. The samples from the extruder were palletized into the granules. The granules were heated at 200°C for 1 h, and then formed into a panel by press (10.5 MPa) for 5 h using the hot press equipment provided by CARVER., USA.

To investigate the effects of CNFs on the crystalline structure and properties of nanocomposites, the nanocomposites with the addition of 0.5, 1, and 3 wt % CNFs and the UHMWPE/LDPE blend without CNFs were prepared.

### Characterizations of the materials

The differential scanning calorimetry (DSC) analysis was performed on TA Instruments DSC Q1000. The samples of 3–5 mg in weight were heated from 25 to 200°C at the rate of 10°C/min, then cooling down to the 25°C at the rate of 10°C/min and heated from 25 to 200°C at the rate of 10°C/min again. The crystal-

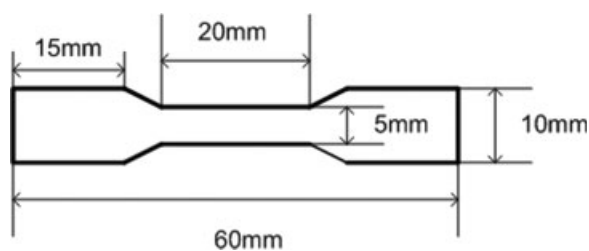


Figure 2 Tensile test specimen geometry, thickness  $\approx$  4 mm.

line structure of carbon nanocomposites was studied by X-ray diffraction (XRD) analysis using the Power Diffractometer Phillips X'Pert MPD system. The wavelength of X-ray was 0.1542 nm. All XRD data were collected from  $2\theta = 5\text{--}35^\circ$  with a step interval of  $0.02^\circ$ .

The mechanical properties were measured by a universal testing machine (Q-TEST, MTS) with a 5-kN load cell. The compression-molded panels with different loadings of CNFs were cut into specimens with dumb-bell shape showed in Figure 2. All the specimens were tested at the rate of 2.5 mm/min. The gauge length is 4 mm. The tensile strength and modulus were obtained from average the values of specimens. The morphology of fracture surfaces after tensile test was observed by the JEOL JSM-6300 scanning electron microscope (SEM).

Dynamic mechanical analysis (DMA) using Q800, TA Instruments, in three-point bending mode was used to measure the dynamic mechanical properties of the nanocomposites. Rectangular specimens of  $60\text{ mm} \times 10\text{ mm} \times 4\text{ mm}$  in three dimensions were cut from compression-molded panels for DMA test. The initial load is 0.01N and amplitude is 20  $\mu\text{m}$ . The samples were ramped from room temperature to  $-100^\circ\text{C}$  at  $3^\circ\text{C}/\text{min}$ , equilibrated at  $-100^\circ\text{C}$ , and then heated to  $200^\circ\text{C}$  at  $5^\circ\text{C}/\text{min}$ . From the DMA analysis, storage modulus ( $E'$ ) and damping factor ( $\tan \delta$ ) were obtained.

The thermal conductivity coefficients were measured by the Mathis TC-30<sup>TM</sup> conductivity test system. The cooling time and test duration were 1 h and 10 s, respectively. The thermogravimetical analysis (TGA) was performed on Q500, TA Instruments. The samples were heated up from ambient temperature to  $600^\circ\text{C}$  under nitrogen gas atmosphere. The heating rate is  $10^\circ\text{C}/\text{min}$ .

## RESULTS AND DISCUSSION

### Crystalline structure of carbon nanocomposites

The crystalline, melting temperature and degree of crystallinity of the polymer matrix nanocomposites were studied by the DSC test. The DSC test was in

the heat/cool/heat procedures. The samples were heated from 25 to  $200^\circ\text{C}$  at the rate of  $10^\circ\text{C}/\text{min}$  in the first heating scan, and then cooling down to the  $25^\circ\text{C}$  at the rate of  $10^\circ\text{C}/\text{min}$  for crystallization, followed by second heating procedure from 25 to  $200^\circ\text{C}$  at the rate of  $10^\circ\text{C}/\text{min}$ . Figure 3 is the com-

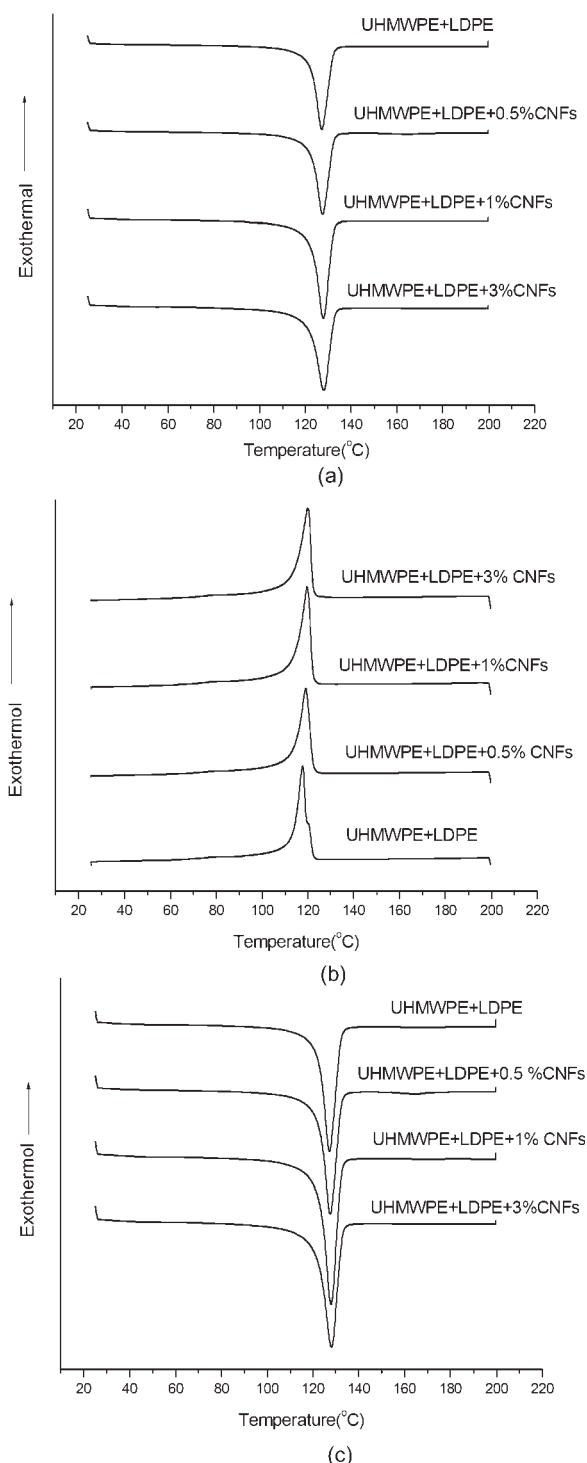


Figure 3 The comparison in the DSC curves of nanocomposites with different loadings of CNFs. (a) first heating (b) cooling (c) second heating.

TABLE I  
The Thermal Parameters Obtained from DSC Curves of Nanocomposites

	First heating			Cooling		Second heating		
	$T_m$ (°C)	$\Delta H_f$ (J/g)	$\Delta\chi$ (%)	$T_c$ (°C)	$\Delta H_c$ (J/g)	$T_m$ (°C)	$\Delta H_f$ (J/g)	$\Delta\chi$ (%)
UHMWPE+LDPE	127.1	151.1	–	117.7	168.5	127.9	168.6	–
0.5 wt % CNFs	127.4	120.5	–20.3	119.0	135.4	128.6	125.8	–25.4
1 wt % CNFs	127.9	144.3	–4.5	119.6	153.2	128.6	148.1	–12.2
3 wt % CNFs	128.1	143.9	–4.8	119.9	144.0	128.3	149.1	–11.6

parison in DSC curves of the polymer nanocomposites in the first heating scan (a), crystallization during cooling (b), and second heating scan (c).

Table I summarizes the thermal parameters obtained from the DSC curves of the polymer matrix and nanocomposites. Melting temperature ( $T_m$ ) and melting enthalpy ( $\Delta H_f$ ) were obtained from the peak temperature and peak area of DSC heating curves, respectively, in Figure 3(a,c). Crystallization temperature ( $T_c$ ) and crystallization enthalpy ( $\Delta H_c$ ) were obtained from the peak temperature and peak area of DSC cooling curves in Figure 3(b). The relative variation values in degree of crystallinity ( $\Delta\chi$ ) were calculated from the heat of fusion with the following expression:

$$\Delta\chi = \frac{\Delta H_f - \Delta H_0}{\Delta H_0} \times 100\%$$

where,  $\Delta H_0$  is the heat of fusion of UHMWPE/LDPE blends.

The melting temperature ( $T_m$ ) in the first heating scan had no visible change with the addition of CNFs. The melting enthalpy ( $\Delta H_f$ ) values of the nanocomposites in first heating scan were obviously lower than that of the polymer blend matrix. The variation in  $\Delta H_f$  in the first scan caused the difference in the  $\Delta\chi$  values, which are related to the degree of crystallinity. According to the values of  $\Delta\chi$ , we found that the degree of crystallinity in nanocomposites with 0.5, 1, and 3 wt % CNFs were reduced by 20.3, 4.5, and 4.8%, respectively, compared with that of the UHMWPE/LDPE blend. In the cooling process, the variation in crystallization temperature ( $T_c$ ) was also not obvious. The crystallization enthalpy ( $\Delta H_c$ ) values of nanocomposites were decreased compared with that of the polymer blend. The nanocomposite with 0.5 wt % had the lowest  $\Delta H_c$  value (135.4 J/g). In the second heating scan, the variation in  $T_m$  is not obvious. The values ( $\Delta\chi$ ) showed the degree of crystallinity in nanocomposites with 0.5, 1, and 3 wt % CNFs that were reduced by 25.3, 12.2, and 11.6%, respectively, compared with that of the polymer blend matrix. The variation in  $\Delta\chi$  values in the second scan was consistent with that in the first heating scan.

Therefore, it can be concluded that the addition of CNFs made little effect on the crystalline structure and melting temperature, but caused a nonlinear decrease in the degree of crystallinity of the polymer nanocomposites. Generally, the CNFs affect the degree of crystallinity through nucleation and crystal growth. With the addition of CNFs into the UHMWPE/LDPE blend, the CNFs as the effective heterogeneous nuclei could increase the amount of nuclei in the crystallization process, which may increase the degree of crystallinity in the nanocomposites. At the same time, the friction between the CNFs and polymer chains hindered the mobility of polymer chains in the crystal growth, which could decrease the degree of crystallinity in the nanocomposites.<sup>21</sup> It is assumed that the hindering effect caused by CNFs in crystal growth is dominant. Therefore, the degrees of crystallinity in the three kinds of nanocomposites were lower than that of the polymer blend matrix. This dominant hindering effect was also found in the polypropylene reinforced by CNTs,<sup>22</sup> which suggested that the nanofillers acting as restriction sites hindered polymer segments from forming highly order arrangements, and as a result, the nanofillers decreased the degree of crystallinity in the nanocomposites.

According to the assumption that the hindering effect of CNFs is dominant during crystal growth process, the small content of CNFs should have a high degree of crystallinity associated with the high content of CNFs. However, the DSC results showed the degree of crystallinity in nanocomposite with 0.5 wt % CNFs was lower than those of the nanocomposites with 1 and 3% CNFs, and nanocomposites with 1 and 3% CNFs had the similar degree of crystallinity (see  $\Delta\chi$  values in Table I). It is speculated that the CNFs could cause other changes in the structures of nanocomposites, which influenced the degree of crystallinity in this nanocomposite. These structural changes in the nanocomposites were further studied by the XRD and SEM test.

Figure 4 exhibits the XRD patterns of nanocomposites with different loadings of CNFs. The diffraction peaks at 21.6°, 24.0°, and 30.0° of  $2\theta$  are assigned to the (110), (200), and (020) crystal planes of polyethylene. The XRD patterns of the nanocomposites have

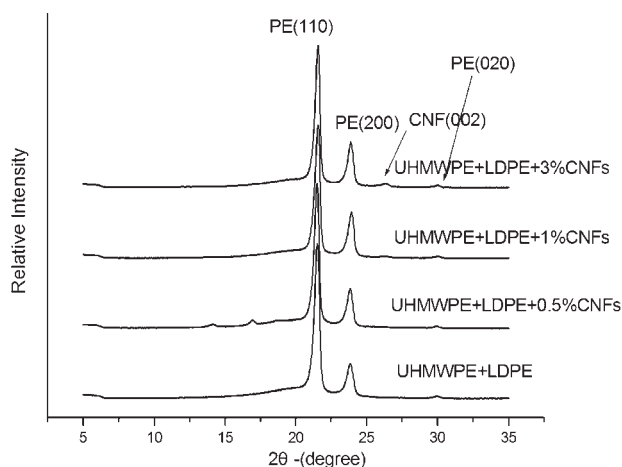


**Figure 4** XRD patterns of nanocomposites with different loadings of CNFs.

another diffraction peak at about  $26.3^\circ$  of  $2\theta$ , which is assigned to the (002) crystal plane of graphitic carbon. The diffraction peak of graphitic carbon is not obvious because the diffraction peak intensity of polyethylene is much higher than that of the graphitic carbon. The diffraction peak intensity is associated with the weight percent of nanocomposite components. In this study, the maximum weight percent of CNFs is only 3 wt %, therefore, the diffraction peak intensity of graphitic carbon is much smaller than others.

To characterize the crystalline structure of nanocomposites, the crystalline size ( $D_{hkl}$ ) vertical to the diffraction planes was calculated by Scherrer's equation:

$$D_{hkl} = \frac{\lambda}{H \times \cos\theta}$$

The space between different diffraction planes ( $d_{hkl}$ ) was calculated by Bragg's equation:

$$D_{hkl} = \frac{n\lambda}{2 \sin\theta}$$

where,  $\lambda$  is the X-ray wavelength used in XRD test, 0.1542 nm;  $H$  is the half high width of diffraction peak;  $\theta$  is the Bragg angle; Table II shows the calculation results from XRD patterns of nanocomposites with different loadings of CNFs.

The  $2\theta$  values of (110) and (200) crystal planes in Table II indicated that there was no obvious shift of all diffraction peak positions with the addition of CNFs. Both  $D_{hkl}$  and  $d_{hkl}$  values remain invariant, implying that the addition of CNFs had negligible influence on the crystalline size of the polymer blend. From the studies of crystallization morphology, it can also be found that the loading of CNFs could increase the degree of crystallinity but make little effect on the crystalline size.

### Mechanical properties

Mechanical properties of the polymer blend and nanocomposite samples with different loadings of CNFs were studied by tensile tests. Table III shows the results obtained from the tensile tests.

It is observed in Table III that the tensile strength of nanocomposites was enhanced with increasing loading of CNFs. The maximum of 38% increase in tensile strength was obtained with an addition of 3 wt % CNFs. It is indicated that the CNFs could improve the tensile strength of UHMWPE/LDPE blend effectively. However, the increase in tensile strength is nonlinear. The increase value (38%) in tensile strength of nanocomposites with 3 wt % nanocomposite was just little more than the increase value (35%) in tensile strength of nanocomposites with 1 wt % nanocomposite.

The modulus of the nanocomposite with an addition of 0.5 wt % CNFs was decreased compared with the UHMWPE/LDPE blend. But the modulus of nanocomposites with loadings of 1 and 3 wt % CNFs were increased. The variation in modulus was influenced by multifactors. One of these factors is the degree of crystallinity. Tensile modulus of the matrix polymer could be increased with the improvement in degree of crystallinity. Another factor is the concentration of CNFs due to their high tensile modulus. The nanocomposites with an addition of 0.5 wt % CNFs had the lowest degree of crystallinity (Table I) and the lowest concentration of CNFs, which led to the lowest tensile modulus in all specimens. When more CNFs were involved, reinforcement effects from CNFs on the modulus are more obvious. Therefore, the modulus of the nano-

**TABLE II**  
Calculated Results from XRD Patterns of Nanocomposites with Different Loadings of CNFs

Sample	$2\theta$ ( $^\circ$ )		$H$ ( $^\circ$ )		$D_{hkl}$ (nm)		$d$ (nm)	
	110	200	110	200	110	200	110	200
Polymer blend	21.58	23.86	0.42	0.52	0.37	0.30	0.41	0.37
Nanocomposite with 0.5 wt % CNFs	21.58	23.86	0.42	0.53	0.37	0.30	0.41	0.37
Nanocomposite with 1 wt % CNFs	21.58	23.95	0.45	0.56	0.35	0.28	0.41	0.37
Nanocomposite with 3 wt % CNFs	21.58	23.95	0.42	0.53	0.37	0.30	0.41	0.37

**TABLE III**  
**The Tensile Test Results of the Polymer Matrix and Nanocomposites**

Sample	Tensile strength (MPa)	Gain in strength (%)	Tensile modulus (MPa)	Gain in modulus (%)
Polymer matrix	19.2 ± 2.1	–	136.2 ± 4.3	–
0.5 wt % CNFs	23.6 ± 0.8	23	131.8 ± 8.9	–3
1 wt % CNFs	25.9 ± 0.5	35	141.6 ± 1.9	4
3 wt % CNFs	26.4 ± 0.8	38	157.1 ± 16.3	15

composite with addition of 3 wt % CNFs is the highest. The fracture surfaces of the nanocomposite samples after tensile tests were studied in the SEM micrographs.

The morphology of fracture surfaces showed the dispersion of CNFs and the phases of the components in the nanocomposites, which could directly affect the mechanical properties of the nanocom-

posites. Figure 5(a) is the SEM image of the UHMWPE/LDPE blend fracture morphology, which shows some small granules dispersed in the fracture flake layer. These small granules are the infused UHMWPE granules similar to those shown in Figure 1. It is known that UHMWPE has long polymer chains, the molecular weight of UHMWPE ( $3.5 \times 10^6$  g/mol) being much bigger than that of LDPE (6

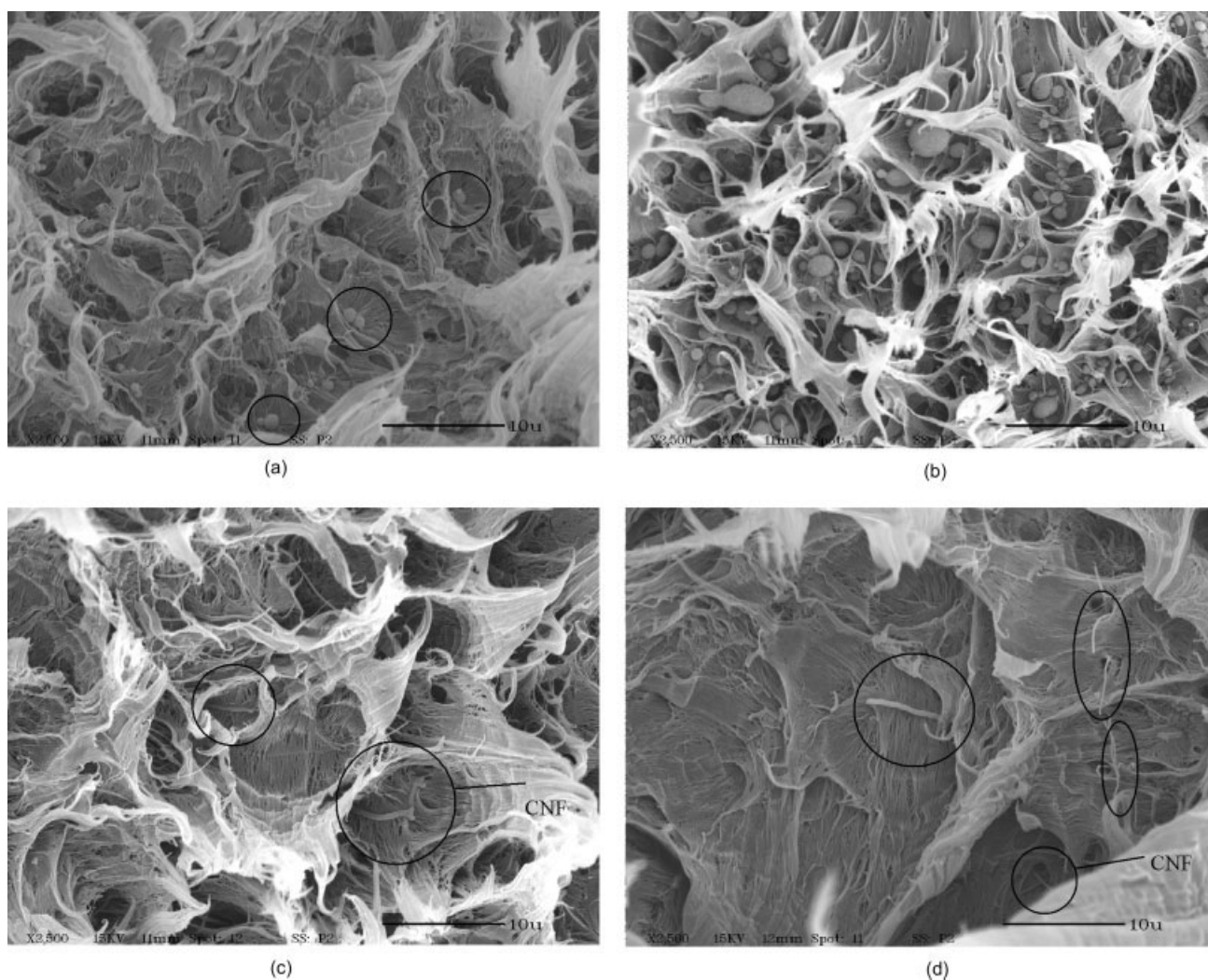


**Figure 5** Fracture surfaces of nanocomposite samples after tensile tests (a) UHMWPE/LDPE blend; the granules were highlighted by the three circles, (b) nanocomposites with 0.5 wt % of CNFs; numerous UHMWPE granules existed, (c) nanocomposite with 1 wt % of CNFs; the CNFs were highlighted by the two circles, (d) nanocomposite with 3 wt % of CNFs; the CNFs were highlighted by the four circles.

$\times 10^4$  g/mol). In the processing of UHMWPE/LDPE blends by the twin-screw extruder, the polymer chains of UHMWPE are only slightly untangled with each other. Therefore, UHMWPE could have incomplete melting during the processing. Many studies have found this phenomenon. Partial dissolution of UHMWPE existed at the processing temperature of 250°C in twin-screw extruder, which could cause many "fisheyes" in the UHMWPE/HDPE film.<sup>23</sup> The UHMWPE dissolved up to about only 3 wt % in the UHMWPE/HDPE blend.<sup>20</sup> Figure 5(b) shows that the amount and the bulk of the infused UHMWPE granules was increased with the addition of 0.5 wt % of CNFs. It is known that graphite materials are solid lubricates. The possible explanation for this phenomenon is that the small amount of CNFs caused a lubricate effect in the twin-screw extruder which decreased the shear force inside the extruder, and thus, resulted in less UHMWPE fused. Figure 5(c,d) show that the infused UHMWPE granules disappeared in the nanocomposites with the additions of 1 or 3 wt % CNFs. These results suggest that when more CNFs were involved, the fusion of UHMWPE could be easily realized due to the high thermal conductivity of the CNFs, which implied that thermal conductive effect of CNFs was more dominant than lubricate effect in the nanocomposites with the larger content of CNFs. The addition of CNFs was shown to enhance the thermal conductivity of the polymer blend, which will be discussed in our later study. It was also observed that the CNFs dispersed in the fracture flake layer, which proved that the twin screw-extruder has the good properties in processing of nanocomposites.

The different fracture morphology of UHMWPE in the blend and nanocomposites with 0.5, 1, and 3 wt % were obvious in Figure 5. The UHMWPE/LDPE

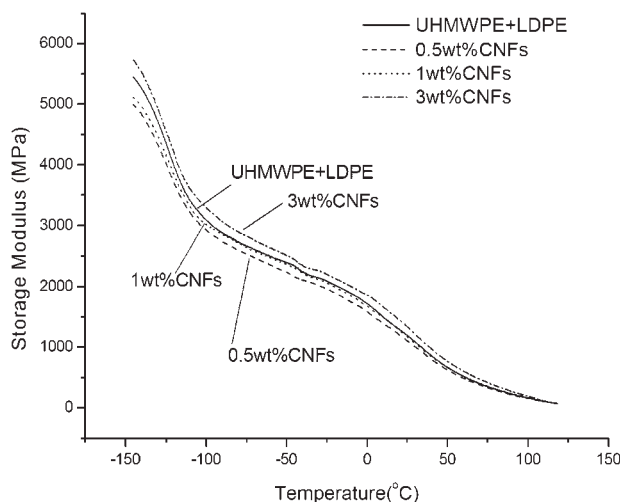


**Figure 6** The storage modulus of the nanocomposites and UHMWPE/LDPE blends.

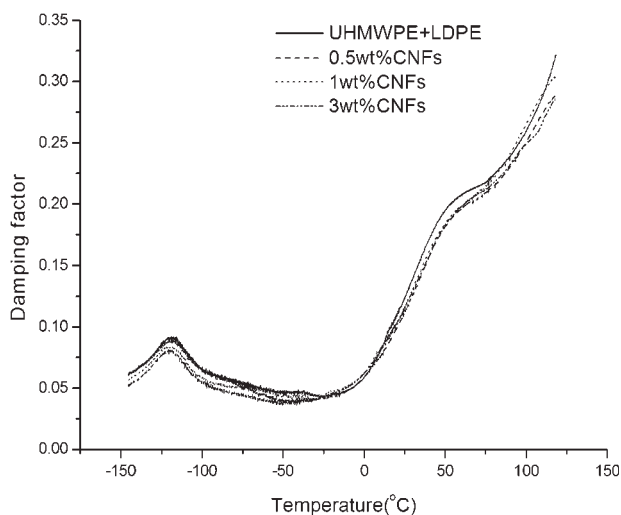


**Figure 7** Damping factor of nanocomposites and UHMWPE/LDPE blends.

blends had few infused UHMWPE granules. The nanocomposite with the loading of 0.5 wt % CNFs had the most infused UHMWPE granules. The nanocomposites with additions of 1 and 3 wt % CNFs did not show visible infused UHMWPE granules. The variation of infused UHMWPE granules could affect the degree of crystallinity of the nanocomposites directly. The infused UHMWPE granules are hard to be crystallized because the chains had little mobility. Therefore, the large amount of infused UHMWPE granules could increase in the size of amorphous regions and decrease the degree of crystallinity in the nanocomposites. The existence of infused UHMWPE granules can be the reason why the degree of crystallinity of the nanocomposite with 0.5 wt % of CNFs was much lower than that of the other nanocomposites and the UHMWPE/LDPE blend. The variation in the amount of the infused UHMWPE granules was also consistent with the results of tensile modulus in Table III, i.e., the infused UHMWPE decreased the tensile modulus of the nanocomposites with 0.5 wt % CNFs through decreasing the degree of crystallinity.

### Dynamic mechanical properties

DMA analysis was applied to study the dynamic mechanical properties including storage modulus ( $E'$ ) and damping factor ( $\tan \delta$ ) shown in Figures 6 and 7, respectively.

Figure 6 shows the storage modulus as a function of temperature of the nanocomposites and the UHMWPE/LDPE blend. The storage modulus of the nanocomposites with additions of 0.5 wt % CNFs was slightly decreased and the nanocomposite with 1 wt % CNFs had no significant change compared with UHMWPE/LDPE blend. It can also be seen

that the storage modulus of the nanocomposites with an addition of 3 wt % CNFs was slightly improved. The storage modulus is related to the degree of crystallinity and molecular chain mobility of the amorphous regions.<sup>24</sup> According to the DSC results in Table I, the addition of CNFs decreased the degree of crystallinity, and thus, decreased the storage modulus. On the other hand, the CNFs could also hinder the mobility of polymer chains in amorphous regions, which could increase the storage modulus. Therefore, for the semicrystalline polymer blends, the differences in the storage moduli are not significant due to the competitive effects of CNFs on the both crystalline and amorphous phases in the materials.

As the melting temperature is approached, the difference between the storage modulus of the nanocomposites and UHMWPE/LDPE blend decreased gradually. At high temperature, the crystallization region of the nanocomposites was destroyed, so the storage modulus of nanocomposites depended only on the intrinsic storage modulus of the matrix.

In the Figure 7, the addition of CNFs did not significantly affect the damping factor ( $\tan \delta$ ) of the polymer blend. It is also observed that the glass transition temperature was negligibly affected by the addition of CNFs. The damping factor of the nanocomposites depends on the dissipated energy caused by friction between the matrix–matrix and fiber–matrix. The small loading of CNFs in experiments made negligible effect on the dissipated energy.

### Thermal conductivity and stability

Figure 8 shows the variation of the thermal conductivity coefficient with the addition of CNFs. It is obvious that the thermal conductivity coefficients of

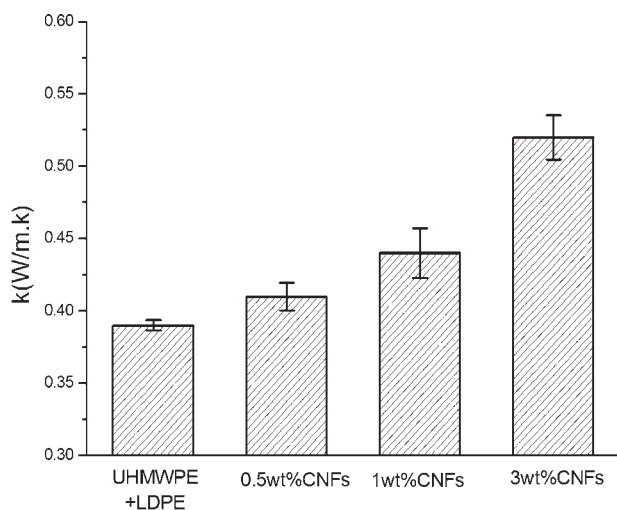


**Figure 8** Variation of thermal conductivity coefficient with an addition of CNFs.

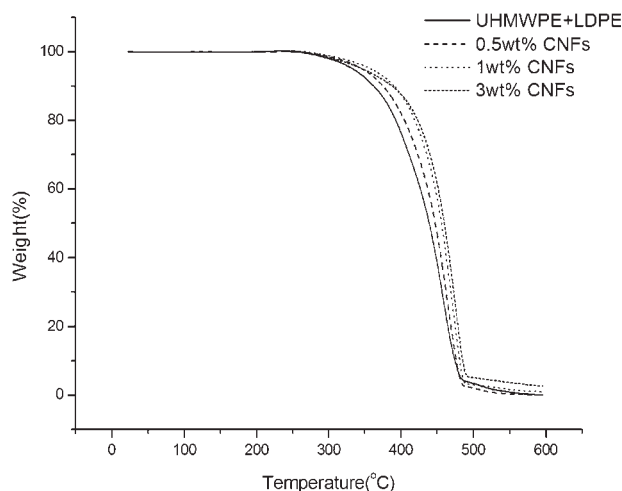


**Figure 9** TGA curve of nanocomposites and UHMWPE/LDPE blends under nitrogen.

the nanocomposites were increased with the addition of CNFs. The explanation is that CNFs have good thermal conductivity which caused the enhancement in thermal conductivity of the nanocomposites. The thermal conductivity coefficient of the nanocomposite with 3 wt % CNFs is highest, which indicates that the dispersal of CNFs is uniform.

The TGA curves of the nanocomposites and the UHMWPE/LDPE blend are shown in Figure 9. It can be found that the thermal stability of nanocomposites was slightly enhanced with the increasing addition of CNFs, the nanocomposites with 3 wt % CNFs had the maximum value of thermal stability. This enhancement was as a result of the restriction effect of CNFs on polymer chains and good thermal stability of CNF itself.<sup>24</sup> The CNFs also have the good thermal conductivity so that they could distribute the heat in the nanocomposites and retard the degradation of polymers caused by the heat concentration in one region.

### CONCLUSIONS

The lab size twin-screw extruder was initially applied to make the CNFs reinforced a polymer blend, UHMWPE, and LDPE, having very different molecular weights and viscosity in melting state between them, through which the complicated effects of CNFs on the semicrystalline structures and properties were investigated.

It was found that for the semicrystalline structures, the effects on the amorphous phase and crystalline phase are different, and even competitive. The addition of CNFs into the UHMWPE/LDPE blend could influence the degree of crystallization, but made little effort in the crystalline structure of the polymer matrix. The small amount of CNFs



caused an increase in the amount of infused UHMWPE particles in the blends, while the large amount of CNFs exhibited the opposite effects. The tensile strength and modulus of the nanocomposite were increased due to the high strength and modulus of the CNFs. The effects of CNFs on tensile modulus of the nanocomposites were also relative to the existence of the infused UHMWPE particles in the materials. Dynamic mechanical properties of the nanocomposites had slight variation compared with UHMWPE/LDPE blend. The thermal conductivity of nanocomposites had been increased with the increasing loads of CNFs. The thermal stability of nanocomposites was slightly improved by the addition of CNFs.

The authors gratefully acknowledge the support from NASA through grant NNM04AA 62G.

## References

1. Pruitt, L. A. *Biomaterials* 2005, 26, 905.
2. Baker, D. A.; Hastings, R. S.; Pruitt, L. *Polymer* 2000, 41, 795.
3. Bellare, A.; Cohen, R. E. *Biomaterials* 1996, 17, 2325.
4. Pascaud, R. S.; Evans, W. T.; McCullagh, P. J. J.; FitzPatrick, D. P. *Biomaterials* 1997, 18, 727.
5. Chan, C. M.; Cheng, C. L.; Yuen, M. M. *Polym Eng Sci* 1997, 37, 1127.
6. Thongruang, W.; Balik, C. M.; Spontak, R. J. *J Polym Sci Part B: Polym Phys* 2002, 40, 1013.
7. Wu, Q. Y.; Wang, X.; Gao, W. P.; Hu, Y. L.; Qi, Z. N. *J Appl Polym Sci* 2001, 80, 2154.
8. Anderson, B. C.; Bloon, P. D.; Baikerikar, K. G.; Sheares, V. V.; Mallapragada, S. K. *Biomaterials* 2002, 23, 1761.
9. Deng, M.; Shalaby, S. W. *Biomaterials* 1997, 18, 645.
10. Fang, L.; Leng, Y.; Gao, P. *Biomaterials* 2006, 27, 3701.
11. Finegan, I. C.; Tibbetts, G. G.; Gibson, R. F. *Compos Sci Technol* 2003, 63, 1629.
12. Lozano, K.; Yang, S. Y.; Zeng, Q. *J Appl Polym Sci* 2004, 93, 155.
13. Mahfuz, H.; Adnan, A.; Rangari, V. K.; Jeelani, S.; Jang, B. Z. *Compos A* 2004, 35, 519.
14. Hasan, M. M.; Zhou, Y. X.; Jeelani, S. *Mater Lett* 2007, 61, 1134.
15. Chen, X. M.; Yoon, K.; Burger, C.; Sics, I.; Fang, D. F.; Hsiao, B. S.; Chu, B. *Macromolecules* 2005, 38, 3883.
16. Zhou, Y. X.; Pervin, F.; Rangari, V. K.; Jeelani, S. *Mater Sci Eng A* 2006, 426, 221.
17. Ruan, S. L.; Gao, P.; Yang, X. G.; Yu, T. X. *Polymer* 2003, 44, 5643.
18. Chiu, H. T.; Wang, J. H. *J Appl Polym Sci* 1998, 70, 1009.
19. Liu, G. D.; Li, H. L. *J Appl Polym Sci* 2003, 89, 2628.
20. Boscoletto, A. B.; Franco, R.; Scapin, M.; Tavan, M. *Eur Polym Mater* 1997, 33, 97.
21. Lozano, K.; Barrera, E. V. *J Appl Polym Sci* 2001, 79, 125.
22. López-Manchado, M. A.; Valentini, L.; Biagiotti, J.; Kenny, J. M. *Carbon* 2005, 43, 1499.
23. Zuo, J. D.; Zhu, Y. M.; Liu, S. M.; Jiang, Z. J.; Zhao, J. Q. *Polym Bull* 2007, 58, 711.
24. Yang, S. Y.; Taha-Tijerina, J.; Serrato-Diaz, V.; Hernandez, K.; Lozano, K. *Compos B* 2007, 38, 228.